32nd Annual International Conference of the IEEE EMBS
Buenos Aires, Argentina, August 31 - September 4, 2010

Detection of Airway Occlusion in Simulated Obstructive Sleep Apnea/Hypopnea using Ultrasound: an *In Vitro* Study

Mohammad A. Al-Abed, *Student Member, IEEE*, Peter Antich, *Senior Member, IEEE,*
Donald E. Watenpaugh, and Khosrow Behbehani, *Senior Member, IEEE*

***Abstract*—Obstructive sleep apnea/hypopnea Syndrome (OSAHS) is the most common form of Sleep Disordered Breathing (SDB) and it is estimated to affect approximately 6% of US adult population. Various methods have been proposed for the development of inexpensive screening methods to detect SDB to reduce the need for costly nocturnal polysomnography (NPSG). By using the existing air in the airway as an ultrasonic contrast agent, we propose a method to examine the narrowing or occlusion of the airway associated with OSAHS events. We describe here an *in vitro* study that approximates the anatomical and acoustic characteristics of the airway and neck. In this experiment, we simulate the fully open airway as well as apnea and hypopnea events. These *in vitro* studies results show significant differences in the ultrasonic signals acquired from the open airway model versus those from the model depicting apnea and hypopnea events. Therefore, the findings provide a foundation for development of an ultrasound system to detect SDB *in vivo*.**

I. Introduction

OBSTRUCTIVE- Sleep Apnea/Hypopnea Syndrome is a sleep disorder, characterized by repetitive pharyngeal collapse. It is prevalent in 6% or more of the middle age population [1]. Patients diagnosed with OSAHS have high incidence of obesity, and exhibit increased risk of hypertension, ventricular failure, and stroke. An association between OSAHS and high morbidity and mortality due to cardiovascular and cerebrovascular causes has been established [1-3]. Patients with OSAHS suffer from fragmented sleep, habitual snoring, morning headaches, and depression. Risk of auto accidents for OSAHS patients equals about seven fold that of controls without OSAHS [2].

Obstructive apneas consist of complete occlusion of the airway at the pharynx, causing a cessation of airflow for ten seconds or more with continuing respiratory effort despite the occlusion. Hypoapnea is manifested by a decrease of 50% or more in the airflow for ten seconds or more, due to the narrowing of the airway at the pharynx [4]. An average of five events or more in an hour of sleep is considered clinically significant, and therefore worthy of medical intervention. This average measurement is called the Apnea/Hypopnea Index (AHI) [3].

In-laboratory nocturnal polysomnography (NPSG) is the gold standard for diagnosis of OSAHS. However, due to the limited number of accredited sleep labs, and the expense of sleep studies, OSAHS may be significantly under-diagnosed [1]. Inexpensive, convenient, yet reliable methods for diagnosis of SDB are highly desired. The current methods that have been developed for diagnosis and large-scale screening for SDB have focused on markers of physiological responses associated with events of airway occlusion, such as sympathoexcitatory or cardiovascular reactions.

In this paper, we examine an ultrasonic *in vitro* airway and neck model that replicates episodes of airway restriction or closure. The eventual goal is to quantify the instance and severity of occlusion using ultrasonic transducers placed on the neck surface. We describe the anatomical parameters and constraints taken into consideration for the design of the model, the experimental set-up, ultrasonic operation, data collection protocol, and results of apnea and hypopnea simulation with this model.

II. Methodology

A. Site of Airway Obstruction

The site of occlusion of the airway during obstructive sleep apnea events differs slightly, with intra- and inter-subject variations. However, most studies, irrespective of the technique used to localize the occlusion, indicate that the main site of occlusion is the oropharynx, sometimes with extension to the laryngopharynx [5]. Figure 1 shows an illustration of the sagittal view of the head and neck, showing the upper airway and its segments. The oropharynx is the segment of the airway that extends from the end of hard palate to the epiglottis, and includes the soft palate and posterior tongue. The end of the oropharynx is defined by a horizontal line drawn from the disk between the C2 and C3 cervical vertebrae [5].

Manuscript received April 23, 2010. This work was supported in part by a grant from the U.S. Department of Energy.

M. A. Al-Abed is a Ph.D. student with the Department of Bioengineering, the University of Texas at Arlington, Arlington, TX 76010 USA (phone: 817-272-2249; fax: 817-272-2251; e-mail: mohammad@uta.edu).

P. Antich is professor and chair of the Radiology Department and the Bioengineering Program at the University of Texas Southwestern Medical Center in Dallas, Dallas TX 75390 USA (e-mail: Peter.Antich@UTSouthwestern.edu).

D. E. Watenpaugh is a physiologist and sleep medicine specialist with Sleep Consultants, Inc., Fort Worth, TX, 76104 USA.

K. Behbehani is a professor and chair of the Department of Bioengineering Department, the University of Texas at Arlington, Arlington, TX 76010 USA (e-mail: kb@uta.edu).

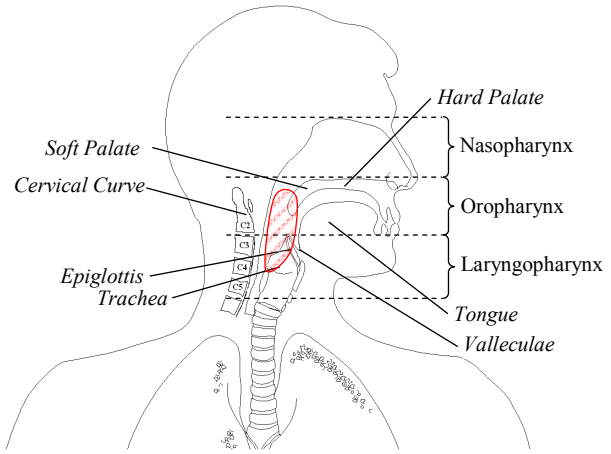

Fig. 1. Sagittal illustration of the head and neck showing the anatomy of the airway. The shaded area represents the portion of upper airway where the occlusion during obstructive sleep apnea events occurs.

B. Significance of the Anatomical Dimensions of the Neck and Airway at the Site of Obstruction

Anatomical structure and dimensions of the neck and upper airway have been correlated with risk and severity of SDB. Larger neck circumference [6], longer length of the upper airway [7], increased thickness of the lateral pharyngeal wall [8], decreased cross-sectional area of the upper airway at the oropharyngeal level [9, 10], and decreased total volume of the airway [10, 11] all correlate with increased risk of SDB. The airway cross-section at the oropharynx level is oval, with the lateral dimension larger than the anterior-posterior dimension. Table I summarizes anatomical structure dimension of the neck and airway in controls and SDB patients as reported in the literature [6, 11].

TABLE I
TYPICAL ANATOMICAL DIMENSIONS FOR SUBJECT WITH SDB IN COMPARISON TO SUBJECTS WITHOUT SDB (MEAN ± STANDARD DEVIATION)

Anatomical Characteristic	Non-SDB	SDB
Neck Circumference (mm)	390 ± 40	406 ± 50
Airway Cross-sectional Area (mm^2)	146.9 ± 111.7	45.8 ± 17.5
Anterior-Posterior Dimension (mm)	7.8 ± 3.3	4.6 ± 1.2
Lateral Dimension (mm)	16.2 ± 6.8	11.6 ± 4.5
Oropharynx Volume (mm^3)	6051.7 ± 1756.4	4868.4 ± 1863.9

C. Ultrasonic Measurements

Ultrasonic biomedical measurements offer the following advantages: safe, non-invasive, use of non-ionizing radiation, inexpensive, simple to use, and commonly portable [12]. A-mode ultrasound is the simplest application, in which an acoustic signal is produced using a piezoelectric transducer vibrating in the medium to high radio frequency range (500 kHz-10MHz). When the acoustic signal encounters an interface between two media with different acoustic impedances, part of the signal is reflected back, and the other part is transmitted through into the posterior medium. A-mode ultrasound uses the reflected or transmitted signals, their attenuation and temporal delay to locate these interfaces.

In medical applications, the acoustic waves travel through human tissue, encountering different media, such as muscle, fat, air cavities, blood, bone, etc. The ultrasound energy attenuates as it travels through various tissues according to their acoustic impedance.

To calculate the characteristic acoustic impedance of a medium (Z_o), we use (1) [13]:

$$Z_o = \rho c \tag{1}$$

where ρ is the medium density and c is the speed of sound in that medium. Table II shows the acoustic properties of water, air, rubber, and some human tissues [13, 14].

TABLE II
AVERAGE SPEED OF SOUND, DENSITY AND ACOUSTIC IMPEDANCE OF SELECTED HUMAN TISSUES, WATER, RUBBER AND AIR

Medium	Speed of sound [m/s]	Desnity [kg/m^3]	Acoustic Impedance [$10^6 \times kg/m^2/s$] or Megarayls
Air (at 1 atm)	343.3	1.2	0.000412
Pure Water (at 20ºC)	1482.3	998.2	1.479
Pure Water (at 30ºC)	1509.1	995.7	1.503
Silicon Rubber	940	1490	1.401
Muscle (at 37ºC)	1547	1050	1.624
Blood (at 37ºC)	1584	1060	1.679
Fat (at 37ºC)	1478	950	1.404
Bone (at 37ºC)	1960	4030	7.898

When the incident ultrasonic wave encounters an interface between two different media, the amount of reflection vs. transmission depends on the difference in the acoustic impedances between the different media [12]. The reflection and transmission coefficients (α_r and α_t respectively) can be calculated as follows [13, 14]:

$$\alpha_r = (Z_2 - Z_1 / Z_2 + Z_1)^2 \tag{2}$$

$$\alpha_t = 4Z_2Z_1 /(Z_2 + Z_1)^2 \tag{3}$$

where Z_1 is the acoustic impedance of medium proximal to the boundary, and Z_2 is the acoustic impedance of the medium distal to the boundary.

D. In Vitro Experiment Design

An *in vitro* model was designed with dimensions comparable the neck and airway. We used materials that model the acoustic characteristics of the human neck and dimensions. Water is used to mimic tissue since its acoustic impedance similar to human soft tissue, which makes up most of sound pathway in the neck, as evident from Table II. Figure 2 shows a photo of the experiment devices: 1) the *in vitro* model set-up, 2) the ultrasound generator and transducers, and 3) the data acquisition system.

In figure 2, the *in vitro* experiment is made up of a 10-

gallon water tank (E1) with a silicon rubber tube (E2) erected at the center of an acrylic ring with a 457mm inside circumference (E3). The ring, which represents the circumference of a neck of an overweight SDB patient, has a diameter of 145.6mm. The rubber tube represents the airway structure and dimensions in the neck. To make it air-tight, it is sealed and glued to base of the tank at one end, and the other end is connected to a 60cc syringe (E4). The tube has an internal diameter of 7.9mm and 1.6mm wall thickness. The syringe is used to create a vacuum in the tube to cause the tube walls to collapse onto each other.

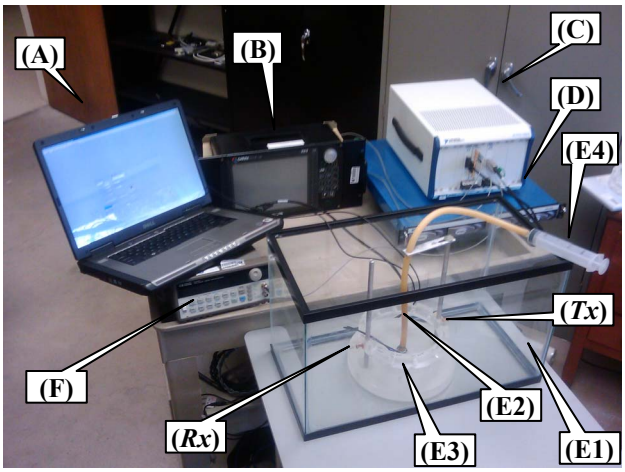

Fig. 2. The *in vitro* experiment set up. (A) is the laptop controlling the data acquisition processes via a LabVIEW interface. (B) The OmniScan *iX* pulse unit. (C) The DAQ unit. (D) External Hard Drive unit for data streaming and storage. (E1-4) represent the neck and airway ultrasonic model: (E4) is the syringe used to create a collapse in the air-filled silicon rubber tube (E2), which is centered on the base of a water tank (E1). An acrylic ring (E3) analogous to the neck circumference has slots that house the ultrasonic transmitter (*Tx*) and receiver (*Rx*). (F) is a function generator that provides the triggering signal for the DAQ.

An 8-channel OmniScan® *iX* UT (Olympus NDT, Quebec, Canada) is used as the source for the ultrasonic pulses (B). Two 6.35mm disk shaped, 2.25MHz, low-Q ceramic PZT-5A ultrasound transducers made by Olympus Panametrics-NDT (State College, PA, USA) are placed in opposite slots in the acrylic rings. One transducer acts as a transmitter (*Tx*), the other acts as the receiver (*Rx*). *Tx* and *Rx* are identical and exchangeable.

The output from the *Tx* and *Rx* is fed into a Data Acquisition (DAQ) system (C) (National Instruments NI PXI-5105, Austin, TX, USA). It is an 8-channel simultaneously-sampled, 60×10^6 Samples/s, 12-bits/Sample data acquisition card. Real-time data are streamed and stored in 1 TB RAID hard drive (NI-8263). The control of the DAQ block is done using National Instruments LabVIEW®. An HP 33120A function generator (Palo Alto, CA, USA) is used as a trigger for the DAQ (F).

E. Data Collection Protocol and Signal Analysis

A fully open airway was mimicked using a fully open rubber tube. By partially removing air from the tube using the syringe (15cc and 30cc), the tube collapses partially to mimic a hypopnea event, whereas a full vacuum causes complete collapse of the rubber tube, mimicking an apnea event. Ultrasonic signals transmitted through and reflected from the tube were collected for these four conditions. The energy in these collected signals was measured.

III. RESULTS

A. Reflection and Transmission Signals

The first detected signal transmitted through to the *Rx*, or reflected back to the *Tx*, arrives and peaks around 98µs after the pulse is generated. As air was removed from the tube, changes in the amplitude of the arriving signal and its delay were recorded. Figure 3 illustrates these observations for the cases when no air was removed (0 cc) as well as three levels of air volume removed from the tube (15 cc through 40 cc).

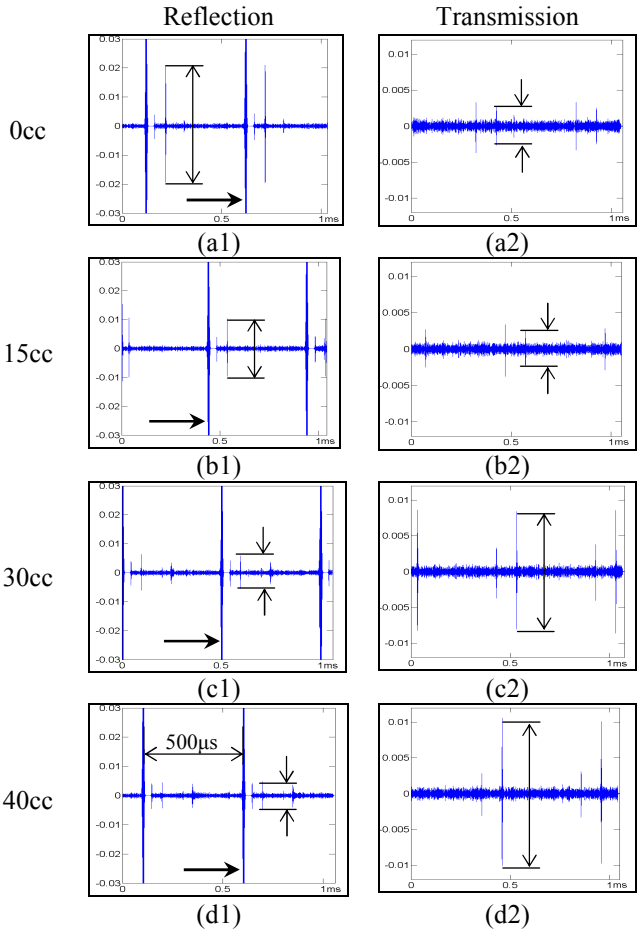

Fig. 3. This figure shows the recorded ultrasonic signals for different airway occlusion models: Reflected (a1) and transmitted (a2) pulses with an open airway model; reflected (b1, c1) and transmitted (b2, c2) pulses with a narrowing airway model; and reflected (d1) and transmitted (d2) pulses with a fully occluded airway model. The horizontal arrow (→) points to the ultrasonic pulse. The temporal separation between the pulses was 500µs, since the pulse repetition frequency (PRF) was 2000 pulses/sec.

B. Energy Computation

We calculated the energy of the arriving signal at the *Tx* and *Rx* terminals for a 30µs window, represented by 180,000

samples. The energy (E_S) is calculated using (4)

$$E_S = \sum_n [s(n)]^2 \quad (4)$$

where *s(n)* is the acquired signal, and n = 1, 2,.., 180,000.

Figure 4 illustrates the average energy for each the transmission and reflections modes with respect to the four simulated airway conditions for which the ultrasonic pulses are shown in figure 3. As noted from figure 4, there is a significant difference in the measured reflected signal energy between fully open, partially open (15 and 30cc), and completely closed tube (40cc); tested at the significance level of $p < 0.05$. There is also significant difference in the measured transmitted signal energy between fully open, partially open (30cc) and completely closed tube (40cc) ($p < 0.05$). However, the transmitted energy between an open tube and a partially open tube at 15cc is not significantly different ($p > 0.05$).

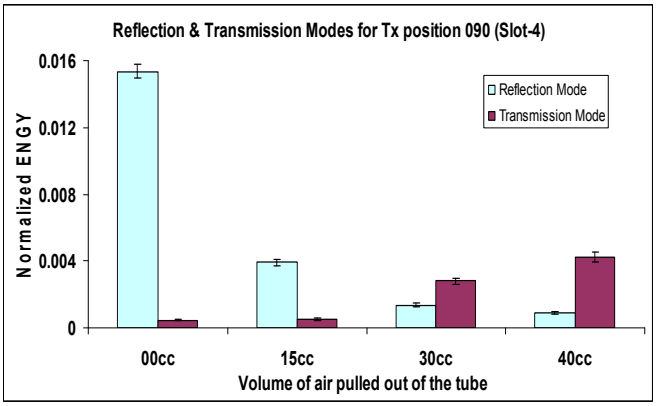

Fig. 4. The mean energy of the Reflection and Transmission modes for simulated open airway (0 cc), simulated hypopnea (15cc and 30cc) and simulated apnea (40cc). Error bars represent the standard deviation.

IV. Discussion

This *in vitro* study aims to explore the feasibility of using ultrasound beam for detecting and quantifying changes in a mechanical model of airway when occlusion occurs. As Table II shows, rubber and water acoustic impedances are closely matched (reflection coefficient, α_r, for the water-rubber interface is 7.3×10^{-4}), whereas there is a mismatch in the acoustic impedance between rubber and air (reflection coefficient, α_r, for the rubber-air interface is 0.999). This is noted in the marked reflected signal in the case when the tube is full of air (figure 3(a1)). As air is removed from the tube, the magnitude of the reflected signal decreases. The amount of reflected signal is minimized when the tube is completely collapsed (figure 3(d1)).

Conversely, the rubber-air acoustic impedance mismatch causes most of the signal to be reflected, and not transmitted (the transmission coefficient, α_t, for the rubber-air interface is 1×10^{-4}). This is seen as the signal transmitted through the tube is minimized when the tube is full of air (figure 3(a2)). The amplitude of the transmitted signal increases as air is removed from the tube, and is maximized when the tube is completely collapsed (figure 3(d2)).

V. Conclusion

We have presented a novel *in vitro* study for the utilization of ultrasonic sensing for the detection of airway narrowing and occlusion that approximates episodes of obstructive sleep apnea/hypopnea. Using acoustic impedance mismatch between water and air, we were able to characterize the existence or lack of air in the simulated airway using transmitted and reflected signals. The use of ultrasound detection of airway occlusion events may offer a simple, cost effective, and specific screening tool for OSAHS. However, this possibility depends on confirmation with *in vivo* studies, which are planned for the near future.

VI. References

[1] T. Young, L. Finn, P. E. Peppard, M. Szklo-Coxe, D. Austin, F. J. Nieto, R. Stubbs, and K. M. Hla, "Sleep Disordered Breathing and Mortality: Eighteen-Year Follow-up of the Wisconsin Sleep Cohort," *Sleep*, vol. 31, pp. 1071-1078, 2008.

[2] P. J. Strollo and R. M. Rogers, "Obstructive Sleep Apnea," *New England Journal of Medicine*, vol. 334, pp. 99-104, 1996.

[3] T. Young, P. E. Peppard, and D. J. Gottlieb, "Epidemiology of Obstructive Sleep Apnea: A Population Health Perspective," *American Journal of Respiratory and Critical Care Medicine*, vol. 165, pp. 1217-1239, 2002.

[4] F. Roux, C. D'Ambrosio, and V. Mohsenin, "Sleep-related breathing disorders and cardiovascular disease," *The American Journal of Medicine*, vol. 108, pp. 396-402, 2000.

[5] A. N. Rama, S. H. Tekwani, and C. A. Kushida, "Sites of Obstruction in Obstructive Sleep Apnea," *Chest*, vol. 122, pp. 1139-1147, 2002.

[6] R. J. Davies, N. J. Ali, and J. R. Stradling, "Neck circumference and other clinical features in the diagnosis of the obstructive sleep apnoea syndrome," *Thorax*, vol. 47, pp. 101-105, 1992.

[7] A. Malhotra, Y. Huang, R. B. Fogel, G. Pillar, J. K. Edwards, R. Kikinis, S. H. Loring, and D. P. White, "The Male Predisposition to Pharyngeal Collapse: Importance of Airway Length," *American Journal of Respiratory and Critical Care Medicine*, vol. 166, pp. 1388-1395, 2002.

[8] K. Liu, W. Chu, K. To, F. Ko, M. Tong, J. Chan, and D. Hui, "Sonographic measurement of lateral parapharyngeal wall thickness in patients with obstructive sleep apnea," *Sleep*, vol. 30, pp. 1503-1508, 2007.

[9] M. A. Ciscar, G. Juan, V. Martínez, M. Ramón, T. Lloret, J. Mínguez, M. Armengot, J. Marín, and J. Basterra, "Magnetic resonance imaging of the pharynx in OSA patients and healthy subjects," *European Respiratory Journal*, vol. 17, pp. 79-86, 2001.

[10] T. Ogawa, R. Enciso, W. H. Shintaku, and G. T. Clark, "Evaluation of cross-section airway configuration of obstructive sleep apnea," *Oral Surgery, Oral Medicine, Oral Pathology, Oral Radiology, and Endodontology*, vol. 103, pp. 102-108, 2007.

[11] R. J. Schwab, M. Pasirstein, R. Pierson, A. Mackley, R. Hachadoorian, R. Arens, G. Maislin, and A. I. Pack, "Identification of Upper Airway Anatomic Risk Factors for Obstructive Sleep Apnea with Volumetric Magnetic Resonance Imaging," *American Journal of Respiratory and Critical Care Medicine*, vol. 168, pp. 522-530, 2003.

[12] J. Quistgaard, "Signal acquisition and processing in medical diagnostic ultrasound," *IEEE Signal Processing Magazine*, vol. 14, pp. 67-74, 1997.

[13] R. S. Cobbold, *Foundations of Biomedical Ultrasound*, 1st ed. New York City, New York: Oxford University Press, 2007.

[14] W. R. Hedrick, D. L. Hykes, and D. E. Starchman, *Ultrasound Physics and Instrumentation*, Fourth ed. St. Louis, MO: Elsevier Mosby, 2005.